ENSO and PDO Influence to Climate Variability in Monsoon Region of Indonesia

E Yulihastin[1,2], N Cholianawati[1], G. A Nugroho[1], T Sinatra[1] and H Satyawardhana[1]

[1]Atmospheric Science Research Group, Faculty of Earth Sciences and Technology, Institut Teknologi Bandung, Indonesia
[2]Center of Atmospheric Science and Technology, National Institute of Aeronautics and Space, Indonesia

E-mail: erma.yulihastin@gmail.com

Abstract. Climate variability can be identified based on two climate parameters: Outgoing Longwave Radiation (OLR) and Precipitable Water (PW). South of Indonesia (2-10^{o}S, 90-15^{o}E) is a rainfall monsoon region with relatively homogeneous characteristics in seasonal variations. However, the region has some certain sensitivities in responding variability from intraseasonal to interannual. Using the method of Empirical Mode Decomposition (EMD), S-Transform and Wavelet for 30 years monthly data of OLR and PW (1980-2011), it was found that both of data indicate signal strengthening after 2010 which is related to Tropical Multi-decadal Mode. Regional response from Intraseasonal to interannual variations confirm that both parameters are sensitive to 1-3 monthly (Intraseasonal Variation) related to MJO, 6 month and 1 year related to monsoon, the 2-7 year variability associated with El Niño Southern Oscillation (ENSO) on short term and medium scale period, whereas 10 yearly due to ENSO in longterm scale period and probably represent the phenomenon of the solar cycle. However it may be suggested that the 15 and 30 year variability would probably corresponded with ENSO and the Pacific Decadal Oscillation (PDO).

1. Introduction

Knowledge of climate variability is more important than the average climate [1]. This is because the value of statistical variability can indicate a variety of important information outside normal climatic conditions such as anomalies, trends and extreme events. The pattern of climate variability in the climate scenario of the changing world is becoming increasingly important to note because the events of weather and climate extremes often acts as a catalyst which is sensitive to climate variability [1].

Climate variability can be identified by two climate parameters, namely Outgoing Longwave Radiation (OLR) [1-7] and Precipitable Water (PW) [8-12] which is a non-stationary data. OLR is associated with wavelengths of the sun (with a wavelength around the wavelength infrared) reflected /emitted by the earth's surface, or reflected by clouds. OLR is the longwave radiation of the sun that is absorbed by the earth's surface and reflected back into space. Some of this long-wave radiation is either retained or trapped in the atmosphere. Thus, the high (low) value of OLR parameters indicates few (many) clouds present in the atmosphere.

Another climate parameter is the PW defined as the amount of water vapor collected in a precipitated column of the atmospheric atmosphere as well as decreased as rainfall when the moisture content in the column has been condensed. The PW value is derived from the specific moisture data, which is a function of pressure and temperature.

The relationship between OLR and PW is negatively correlated, meaning that if a region has a large PW value it means a small OLR value is in the region, and vice versa. This can occur due to high PW value that may indicate more and more clouds are formed as a result of convection activity. When clouds are formed, the atmosphere will absorb more radiation, hence the longwave radiation that is reflected back to space are small so that OLR values will be small or low.

Annual variation of OLR in southern Indonesia is showed by high OLR values indicating the dry season, and vice versa. Meanwhile, the relationship between PW and OLR is negatively correlated with a very high correlation coefficient value of -0.95 [13]. In addition, the annual cycle is clearly identified based on PW and OLR data [13]. However, the opposite relationship between PW and OLR over a longer period of time and variations from year to year in southern Indonesia have not been studied. Yet research on the variation of OLR and PW needs to be done to determine the consistency, sensitivity and change, which is useful as the initial identification of climate change in Indonesia. It due to OLR represented Earth's radiation budget which is a critical component to understand the climate change [14] and precipitable water reflected water vapors as mainly parameter which is contributes at about 50% of the present-day global greenhouse effect [15].

This paper aims to present the results of climate variability studies in the Indonesian monsoon region from the highest (intraseasonal) to the lowest (antartahunan) frequency. In addition, this study also aims to determine the consistency and sensitivity of both parameters in southern Indonesia, in relation to the monsoon phenomenon; i.e. the El Niño Southern Oscillation (ENSO), the 11-yr solar cycle, and the Pacific Decadal Oscillation (PDO).

2. Data and Method

All data in this study has a monthly period ranging from 1980-2011. To examine the periodicity and variance of data used, two methods based on the analysis of the frequency spectrum are deployed: wavelet and S-Transform. Both methods are used so that the resulting frequency spectrum can be interconnected. In addition, to know the variability of the data in more detail by performing the separation of the type of frequency from highest to lowest, the EMD method is performed. The EMD method can also generate data trends indicated by recent IMF results and can provide information on weakening and signaling through wave envelope over the data period. The EMD method is suitable for long-term non-stationary data as is the characteristic of OLR and PW data. The data and methods are described in more detail as follows.

2.1. Data

The main data used are PW data with monthly temporal resolution and 2.5-degree spatial resolution that can be downloaded freely via the following sites: http://www.esrl.noaa.gov/psd/data/gridded/data. ncep.reanalysis.derived.surface. html and OLR data with temporal resolution and 0.05 degree spatial resolution http://www.esrl.noaa.gov/psd/data/gridded/data.interp_OLR.html. PW data is available from 1974 to 2011 while OLR data is available from 1948 to 2011. As supporting data, this study utilize sun spot data obtained from Solar Influences Data Analysis Center (SIDC) http://sidc.oma.be/sunspot-data/ and SOI data Southern Oscillation Index (SOI) http://www.cpc.ncep.noaa.gov/data/indices/. The period of data used is data from January 1980 to December 2011 (30 years).

2.2. Methods

2.2.1 Morlet Wavelet

Wavelet morlet is a wavelet type of complex exponential signal that is modulated with Gaussian window [14].

$$\psi_0(\eta) = \pi^{-1/4} e^{-i\omega_0\eta} e^{-\eta^2/2}$$

Where $\boldsymbol{\psi}$ is the wavelet value at non-dimensional time, while $\boldsymbol{\psi}_0$ is the wave number.

2.2.2 Stockwell Transform Method

The Stockwell transform (S-Transform) produces a representation of the relationship between time-frequency in the time domain. This method is a combination of resolution settings based on frequency and spectral arrangement of real and imaginary values simultaneously [17].

$$S(\tau, f, p) = \int_{-\infty}^{\infty} h(t)\omega(\tau - t, f, p)e^{-j2\pi ft}dt$$

Where p is the parameter that determines the shape and value of f, whereas $\boldsymbol{\psi}$ is the window function of S-transform (Gaussian function with window width depends on its frequency).

$$\omega(t, f, p) = \frac{|f|}{\sqrt{2\pi}p} e^{\frac{t^2 f^2}{2p^2}}$$

2.2.3 EMD Method

The Empirical Mode Decomposition (EMD) principle is to decompose signals based on the direct extraction of signal energy associated with various intrinsic time scales [19]. This technique adaptively decomposes the non-stationary signal into a set of intrinsic oscillatory modes. Components called intrinsic mode functions (IMFs), allow instant component frequency calculations based on the Hilbert transform. Thus, it can potentially localize events in time and frequency.

The starting point of EMD is by reviewing the signal oscillations at a very local level. Given the signal $x(t)$, the effective EMD algorithm can be summarized as follows: (1) identifies all extracts $x(t)$; (2) interpolate between minima and maxima so as to produce some envelope $e_{\min}(t)$ and $e_{\max}(t)$; (3) calculate the average $m(t) = (e_{\min}(t) + e_{\max}(t))/2$; (4) extracting detail $d(t) = x(t) - m(t)$; (5) iteration on residual $m(t)$. The sifting process includes the first iteration of steps 1 through 4 to obtain detailed $d(t)$ signals, then reviewed as zero-mean according to the termination criteria.

Once obtained, the detail is referred to as Intrisic Mode Function (IMF), the corresponding residual is calculated and followed by step 5. The extreme amount will decrease as it moves from one residual to the next, and the overall decomposition is fitted with a finite number of modes. A mode extraction is obtained when the shifting process is complete. Two conditions must be met: (1) the number of extremes and the number of zero-crossings must vary by a maximum of 1; (2) the average between the upper and lower limits of the envelope should be close to zero. Or with sifting process termination criteria: SD value = 0.2 or 0.3.

$$SD = \sum_{t=0}^{T} \left[\frac{|(h_{1(k-1)}(t) - h_{1k}(t))|^2}{h_{1(k-1)}^2{}^{(t)}} \right]$$

3. Result and Discussion

Figure 1 shows areas in southern Indonesia that have seasonally different contrasts in precipitation and OLR patterns especially between the DJF (rainy season) and the JJA (dry season). This distinction in precipitation intensity and the seasonal wind direction is what causes the region to be referred to as

the region with monsoonal rain pattern in Indonesia. Periodicity of OLR and PW data in the region will be further investigated using wavelet analysis.

The wavelet results in **Figure 2a** show the amplitude of OLR anomaly data varying from month to month with values between +2 and -2. **Figures 2b-c** show that the one-year signal is the dominant period of OLR in southern Indonesia. Other emerging signals are 2.5 yr, 5.3 yr and 10.6 yr.

The annual signal is closely related to the monsoon phenomenon. Meanwhile, the 2.5 yr and 5.3 yr signals are influenced by the irregular cycles of ENSO [18, 21-23]. Signal strengths of 2-4 yr and 11 yr on OLR data have the same power spectrum. In addition, for the 2.5 yr, signal strengthening occurred in 1994-2003 while for the 5.3 yr lasted between 1997-2000. For the 10.6 yr, no significant signal strengthening occurs in OLR data. For OLR data variance for 30 years there appears to be no threshold value (**Figure 2d**), which shows that OLR data has a high degree of regularity. It also proved that wavelet method has limitation to decompose OLR signal, so that we need other method which can decompose the non-stationary and non-linear signal data in more details and consistent, i.e. EMD (Empirical Mode Decomposition). It is because wavelets concept considering both low frequency as well as high frequency events simultaneously [19]. In the other hand, the limitation of wavelet morlet which is applied in the current research, depends on the characteristics of the data, also the data border distortion can affect the decomposition process at the two limits of the signal. However, wavelet morlet are the most commonly used for periodic data such as climatology and hydro-meteorology [20].

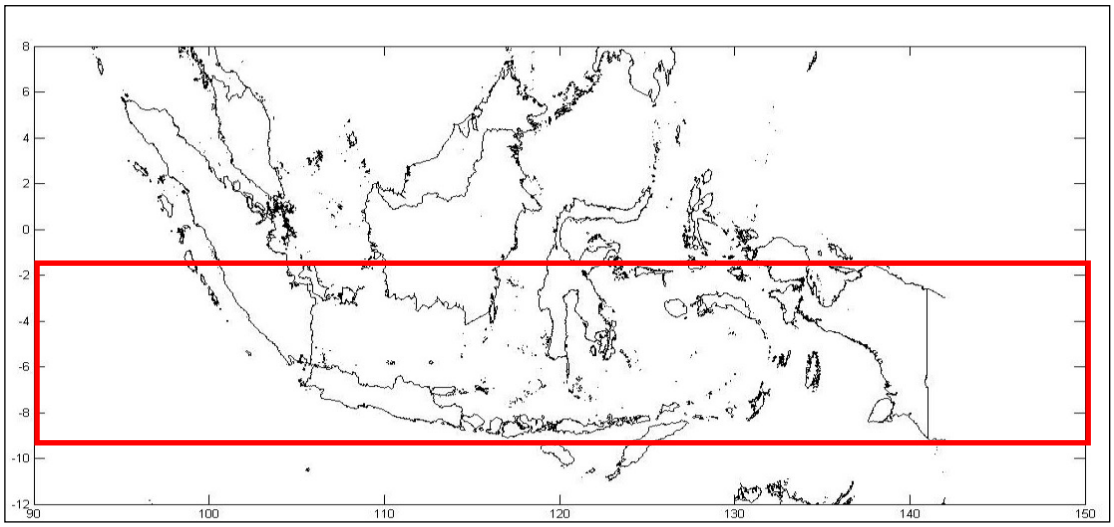

Figure 1. Location of monsoon region of Indonesia

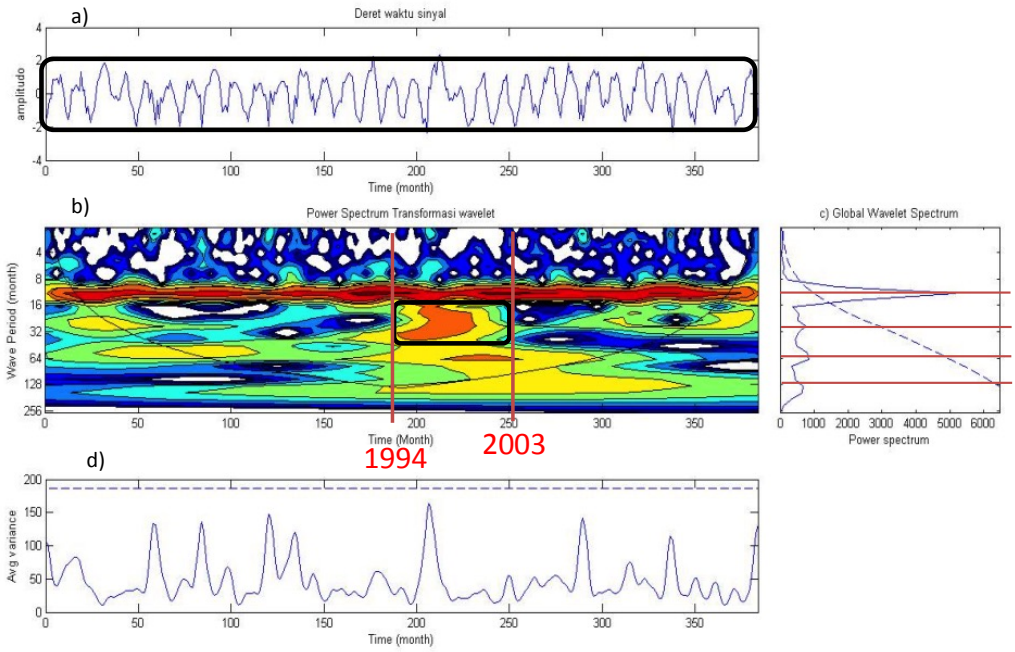

Figure 2. Time series of (a), frequency spectrum (b), and variance (c) based on wavelet method of monthly climatology of OLR (1980-2011)

Meanwhile, in the PW data (Figures 3 (b) and (c)), the dominant periods that emerged were annual, 10.6 yr, 5.3 yr. The 10.6 yr signal strengthened in 1996-2011. For a 2.5 yr, the strongest signal was shown in 1994-2003. The wavelet results for PW data also show that the maximum value of PW after 2010 shows a variance that exceeds its threshold value (Fig. 3 (d)). These findings show different realities to the OLR data.

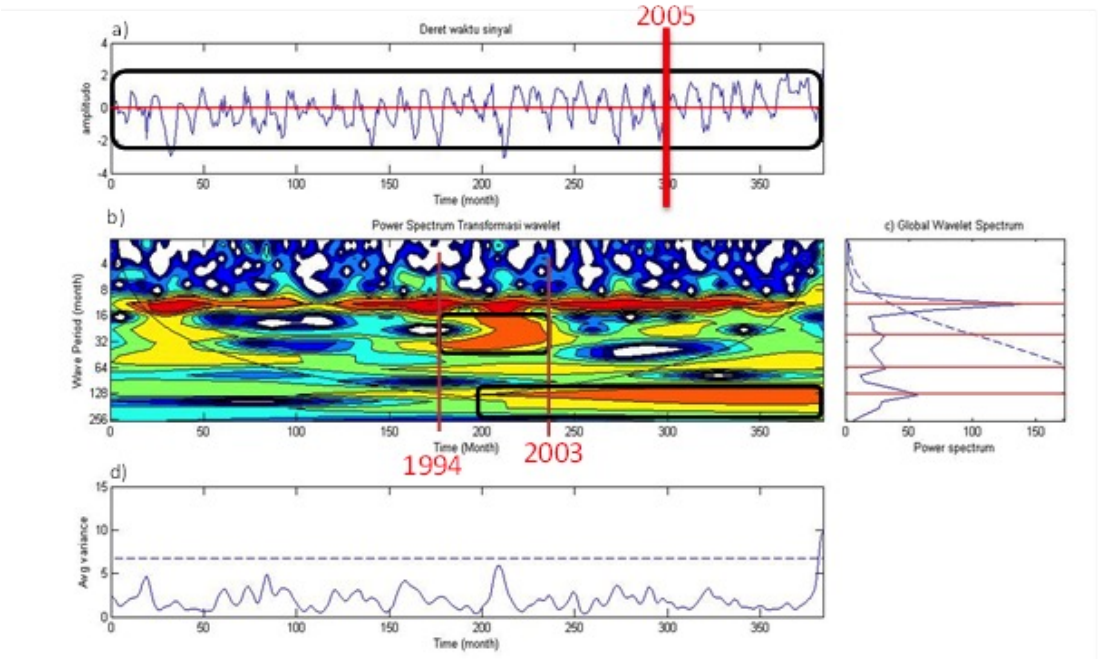

Figure 3. Time series of (a), frequency spectrum (b), and variance (c) based on wavelet method of monthly climatology of PW data (1980-2011)

Different results are exhibited by the S-Transform method, where OLR and PW both show the strongest signal about 5-6 years. This is evident from the five cycles in the OLR data and six cycles in the PW data for 30 years of observation shown by red (**Figure 4**). The frequencies of these five to six times were probably related to the ENSO phenomenon that has an irregular cycle between 2-5 years.

Other signals that appear to have been represented by green and light blue colours, are seen as cycles that always appear throughout the year of observation. This shows the annual cycle associated with monsoon. The interesting point found through the S-Transform method is the dominant signal that appears in 2010 to 2011. Seen in **Figure 4**, both OLR and PW data show the same signal.

Furthermore, to test the consistency of OLR and PW data, cross-correlation between OLR and PW period data were generated from wavelet and S-Transform method. The cross-correlation results describe that both OLR and PW have lag data period of 5 months. This shows the difference in phase calculation between S-Transform and wavelet against OLR and PW data is 5 months. In addition, for the same lag phase (5 months) it seems that the OLR and PW data consistently over 30 years have a correlation that is opposite (**Figure 5**).

Figure 6 explains that by using the EMD method, more detailed signals can be seen in both OLR and PW data. The EMD results in the OLR data show 1-3 months (IMF 1), 6 months (IMF 2), 1.3 years (IMF 3), 2.9 years (IMF 4), 4 years (IMF 5 and IMF 6), 6.4 years (IMF 7), 10.6 years (IMF 8), 15 years (IMF 9) and 30 years (IMF 10). In the PW data, periodic signals are 1-3 (IMF 1), 6 months (IMF 2), 1.3 years (IMF 3), 2.6 years (IMF 4), 3.75 years (IMF 5), 5 years (IMF 6), 7.5 years (IMF 7), 10 years (IMF 8), 15 and 30 years (IMF 9 and 10).

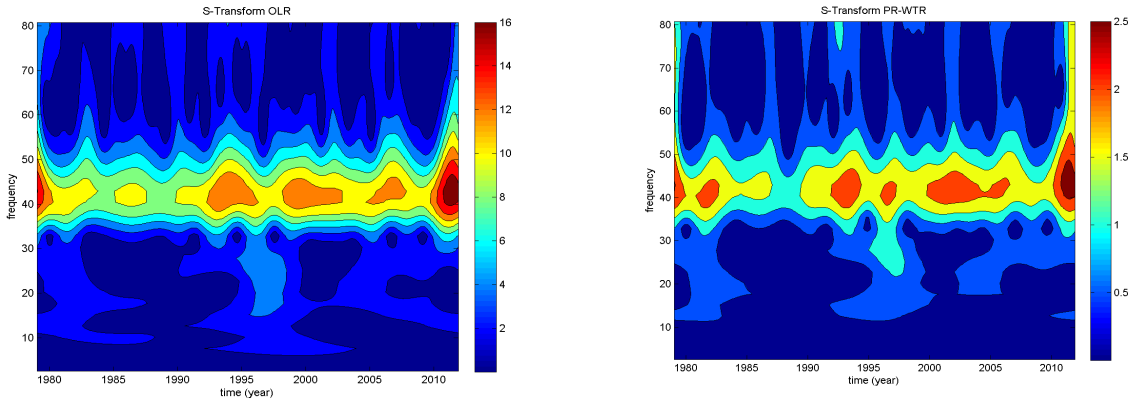

Figure 4. Frequency spectrum based on S-Transform method of monthly climatology of OLR (left) and PW (right) data.

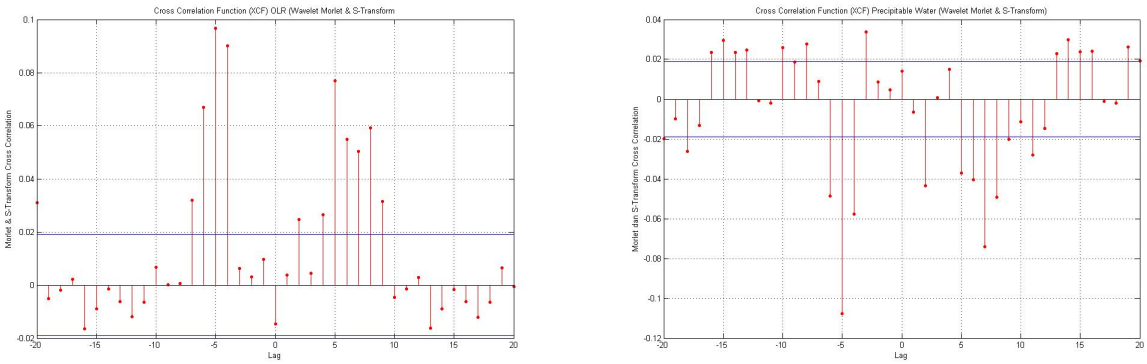

Figure 5. Cross-correlation of OLR (left) and PW (hand right) between frequancy spectrum of wavelet and S-Transform.

IMF 2 and 3 present the 6 monthly and annual signals associated with monsoon activity in southern Indonesia so as to impact the formation of Semi Annual Oscillation and Annual Oscillation. It also appears that signal strengthening for OLR data does not correspond consistently with PW data. Reinforcement of seasonal signals on OLR data generally occurs over a span of two consecutive years (1984-86, 1987-89, 1999-01) except in the period 1992-96 and 2004-08. Similarly, PW data, signal strengthening with the longest duration (8 years) only occurred in 1998-2006. In addition, strong signals took place in 1983-86, 1994-96, 2009-11. For the period 2009-2011, the facts show that there has been a wet in dry season in the Indonesian monsoon region even though in 2009 El Niño occurred in the Pacific Ocean. Some of the events that allegedly can be the cause of the a wet in dry season is because the MJO and tropical cyclone activity that has a higher frequency that is 30-96 days during that period [6].

The Intraseasonal Cycle can be identified through both OLR and PW data through IMF 1 (Figure 6). In fact, the increasing trend of convective activity and the increase in total humidity in atmospheric columns has occurred since 2000 to 2011. This can be demonstrated through the trend pattern of OLR and PW data through IMF 11 (**Figure 7**).

While IMF 4 and IMF 5 are related to the occurrence of ENSO in the Pacific Ocean with a period of 2-4 years, similarly, IMF 6 represents ENSO which has a longer period of 6 years. The relationship between IMF 4 (2 years) and ENSO events is shown in **Figures 8** and **9**. Linear relationships can be identified in the case of strong El Niño in 1997. PW shows a very large value reduction yet at the same time the value of OLR has increased enormously.

The IMF 8 (10 years) is suggested to be related to the 11th annual solar cycle. The 11-yr solar cycle has had an impact on climate change and weather in Europe by altering atmospheric circulation in the North Atlantic Oscillation and Arctic Oscillation indirectly by extending the hot anomalous memory that occurs in the ocean so as to generate a mutual response in the atmosphere [24-25]. It is also possible to explain how the 11yr solar cycle can affect the Asian winter monsoon [22]. In the Pacific Ocean, solar cycles can affect the formation of temperature hiatus conditions due to changes in ocean temperatures in the tropical Pacific [28].

Figure 7 showed IMF 8 (10 years), 9 (15 years), and 10 (30 years) can also be related to the ENSO phenomenon which has low frequency. It proves that ENSO also has lower frequency signals of 13 and 32 years, hereinafter referred to as Multivariate ENSO Index (MEI) as a phenomenon that has a global impact on various climate anomalies, ENSO itself has multi-decadal evolution and dynamics [29-30]. However, there is another possibility of PDO occurrence that were shown by IMF 9 (15 years) and IMF 10 (30 years) through OLR and PW data regarding to previous research that PDO has a period of 16.7 and 32.8 years [29]. Moreover, ENSO and PDO have mutual relations and can modulate each other [31].

This is reinforced by the findings in this study which show that IMF 5 (3-4 years), 6 (5-6 years), and 9 (15 years) are mutually correspondent. Although the same is not shown by IMF 4 (2 years) and IMF 10 (30 years). Thus, the monsoon region in southern Indonesia is merely sensitive to MEI that has 15 years oscillations. Another opinion was expressed by Chelliah which suggests that the 15-20 years relate to another phenomenon called Tropical Multi-Decadal Mode which is evident in precipitation data during the DJF period in the western Pacific region (including Indonesia) [4].

Figure 9 shows that over a 12 year period, two PW wave cycles with peak cycles occurred in 1989-1990 and 2003-2004. Compared with the 11-yr solar cycle data, it appears that at the time of maximum PW during that period, the sun reached the maximum of cycles that occurred in 1989-1992 and 2000-2004.

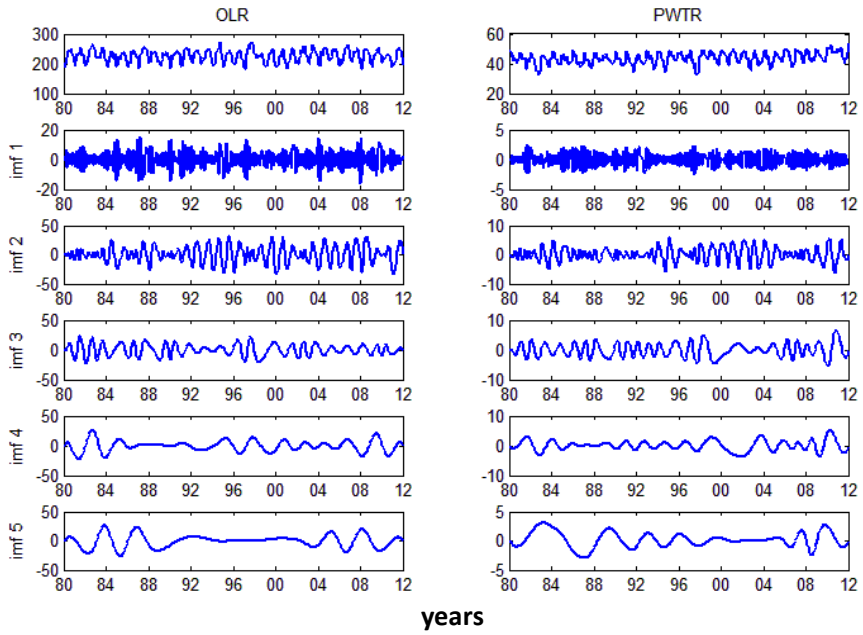

Figure 6. IMF 1-5 based on EMD method for OLR (left) and PW (right) data

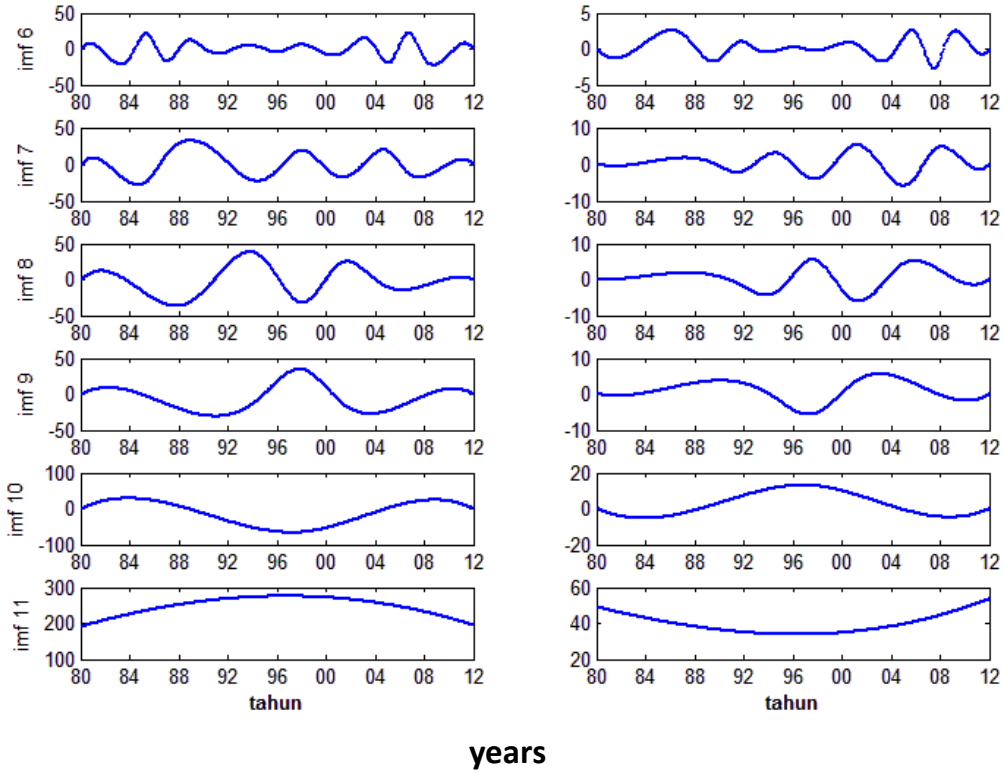

Figure 7. IMF 6-11 based on EMD method for OLR (left) and PW (right) data

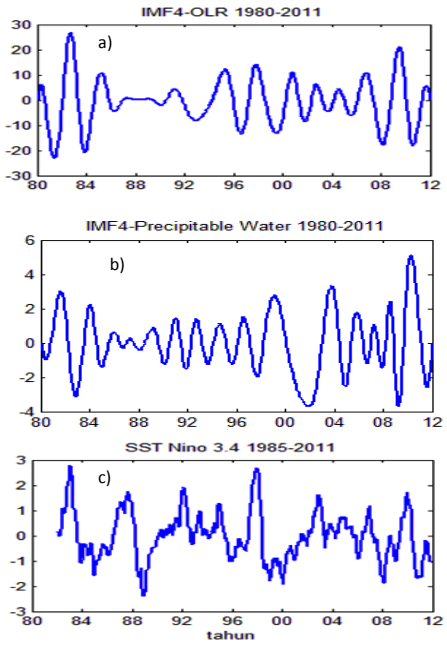

Figure 8. IMF 4 OLR (a), PW (b) compared with SST Nino 3.4 (c)

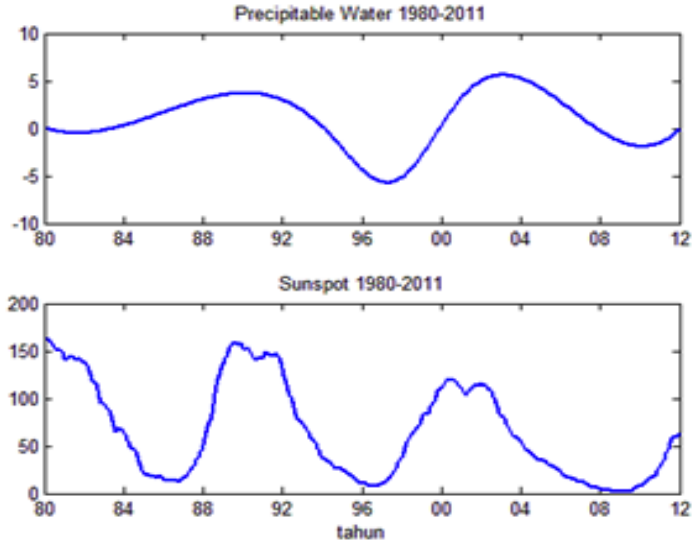

Figure 9. PW and sunspot monthly data of 1980-2011.

4. Conclusion

The wavelet and S-Transform results show that the one-year signal is the dominant period of OLR in southern Indonesia. Other signals that appear are periods of 2, 5, and 10 years. In the wavelets, the 2, 5, and 10 years signals in the OLR data have the same power spectrum. However, in the PW data, the dominant periods that emerged were 1, 10, 2 and 5 years, respectively. The wavelet results for the PW data also show that the maximum value of PW after 2010 shows an anomaly that exceeds the climatological average of the data for 30 years. The S-Transform results of OLR and PW data also clearly show signal strengthening after the 2010 period. While the EMD results show in detail the 1-3 monthly cycles associated with MJO, 6 monthly and 1 yearly associated with monsoon activity, 2-3

yearly related with ENSO short-term, 5-7 years ENSO long periods, 10 years that can be attributed ENSO (EMI) or the 11-yr solar cycle. Signals with lower frequencies of 15 and 30 years can be associated with EMI and PDO phenomena as they can affect each other. This study also found that OLR and PW have consistently for 30 years maintained correlations of the opposite shown from the results of the cross-correlation.

Acknowledgments
The author would like to thank Indonesia Endowment Fund for Education, Ministry of Finance of the Republic of Indonesia for their scholarship in the completion of doctoral studies in Earth Sciences, Faculty of Science and Technology of Earth, Bandung Institute of Technology.

5. References

[1] Katz RW and Brown BG 1992 Extreme events in a changing climate: Variability is more important than averages *Clim. Chang*. **21** 289-302
[2] Lau K-M and Chan PH 1983 Short-term climate variability and atmospheric teleconnections from satellite observed outgoing longwave radiation, part I: Simultaneus relationship *J. Of Atm. Sci.* **40** 2735-2750
[3] Graham NE 1994 Decadal-scale climate variability in the Tropical and North Pacific during the 1970s and 1980s: Observations and model results *Clim. Dyn.* **10** 135-162
[4] Chelliah M and Bell GD 2004 Tropical multidecadal and interannual climate variability in the ncep-ncar reanalysis *J. of Clim.* **17** 1777-1803
[5] England MH, Ummenhofer CC and Santoso 2006 Interannual rainfall extremes over southwest western australia to indian ocean climate variability *J. of Clim* **19** 1948-1969
[6] Waliser DE, Moncrieff MW, Burridge D, Fink AH, Gochis D, Goswami BN, Guan B, Harr P, Heming J, Hsu H.-H., J Christian, Janiga M, Johnson R, Jones S, Knippertz P, M Jose, Nguyen H, Pope M, Serra Y, Thorncroft C, Wheeler M, Wood R and Yuter S 2012 The "year" of tropical convection (May 2008-April 2010) *Bull. Of Amer. Met. Soc.*1189-1218
[7] Trenberth KE, Fasullo J, Smith L 2005 Trends and variability in column-integrated atmospheric water vapor *Clim. Dyn.* **24** 741-748
[8] Amenu GG and Kumar P 2005 NVAP and reanalysis-2 global precipitable water products: Intercomparison and variability studies *Bull of America Met. Soc*. 245-256
[9] Mears CA, Santer BD, Wentz FJ, Taylor KE and Wehner MF 2007 Relationship between temperature and precipitable water changes over tropical oceans *Geoph. Res. Lett.* **34** 1-5
[10] Dessler AE, Zhang Z and Yang P 2008 Water-vapor climate feedback inferred from climate fluctuations, 2003-2008 *Geoph. Res. Lett.* **35** 1-4
[11] Haar THV, Bytheway JL and Forsythe JM 2012 weather and climate analyses using improved global water vapor observations *Geoph. Res. Lett.* **39** 1-6
[12] Bock O, Willis P, Wang J and Mears C 2013 A high-quality, homogenized, global, long-term (1993-2008) doris precipitable water data set for climate monitoring and model verification *J. of Geop. Res.* 7209-72031
[13] Yulihastin E and Hermawan E 2012 Annual migration of monsoon over Indonesia maritime continent based on olr data *J. Tek. Indo.* **35** 1-12
[14] Susskind J, Gyula M, Lena I and Norman GL 2012 Interannual variability of outgoing longwave radiation as observed by AIRS and CERES *J. of Geop. Res.* **117**, 1-8
[15] Schmidt GA, Ruedy RA, Miller RL and Lacis AA 2010 Attribution of the present-day total greenhouse effect *J. of Geop. Res.* **115**, 1-6
[16] Tang YY, Yang LH, Liu J and Ma H 2000 Wavelet theory and its application *World Scient* **36** p 53
[17] Stockwell RG 2007 A basis for efficient of the s-transform *Dig Sig Proc* **17** 371-393
[18] Coughlin K, and Tung KK 2004 Eleven-year solar cycle signal throughout the lower atmosphere *Geophysics Research Letter* **109** DOI:10.1029/2004

[19] Karthikeyan L and Kumar DN 2013 Predictability of nonstationary time series using wavelet and EMD based ARMA models *J. of Hyd.* **502** 103-119
[20] Araghi AA, Mousavi M, Baygi A, Adamowski JB, Malard JB , Nalley DB, and Hasheminia SMA 2015 Using wavelet transforms to estimate surface temperature trends and dominant periodicities in Iran based on gridded reanalysis data *Atm. Res* **155** 52-72
[21] Ren H-L, Jin F-F, Stuecker MF and Xie R 2013 ENSO Regime change since the late 1970s as manifested by two types of ENSO *J. of the Met. Soc. Japan* **91** 835-842
[22] An S-I and Jin F-F 2000 An eigen analysis of the interdecadal changes in the structure and frequency of ENSO Mode *Geophys. Res. Lett.* **27** 2573-2576
[23] An S-I and Wang B 2000 Interdecadal change of the structure of the ENSO mode and its impact on the ENSO frequency *J. Clim.* **13** 2044-2055
[24] Fedorov AV and Philander SG 2000 Is El Niño changing? *Sci.* **288** 1997-2002
[25] Chen W and Zhou Q 2012 Modulation of the arctic oscillation and the East Asian winter climate relationships by the 11-year solar cycle *Adv. In Atm. Sci.* **29** 217-226
[26] Gray LJ, Scaife AA, Mitchell DM, Osprey S, Ineson S, Hardiman S, Butchart N, Knight J, Sutton R, Kodera K 2013 A lagged response to the 11 year solar cycle in observed winter Atlantic/European weather patterns *J. of Geoph. Res. Atm.* **118** 13405-13420
[27] Scaife AA, Ineson S, Knight JR, Gray L, Kunihiko K and Smith DM 2014 A mechanism for lagged North Atlantic response to solar variability *Geop. Res. Lett.* **40** 434-439
[28] Kosaka Y and Xie S-P Recent global-warming hiatus tied to Equatorial Pacific surface cooling nature **501** 403-407
[29] Lee HS, Yamashita T and Mishima T 2012 Multi-decadal variations of ENSO, the Pacific decadal oscillation and tropical cyclones in the Western North Pacific *Prog. in Ocean* **105**, 67-80
[30] Wang S, Huang J, He Y and Guan Y 2014 Combined effects of the Pacific decadal oscillation and El Niño Southern oscillation on global land dry-wet changes *Sci Rep* **4** 1-8
[31] Capotondi A and Sardeshmukh PD 2017 Is El Niño really changing? *Amer. Geop. Uni.* 10.1002/2017GL074515 1-15